ISSN 0023-1584, Kinetics and Catalysis, 2018, Vol. 59, No. 5, pp. 601–609. © Pleiades Publishing, Ltd., 2018.
Original Russian Text © P.V. Markov, G.O. Bragina, G.N. Baeva, A.V. Rassolov, I.S. Mashkovsky, A.Yu. Stakheev, 2018, published in Kinetika i Kataliz, 2018, Vol. 59, No. 5, pp. 591–600.

Highly Selective Pd–Cu/α-Al_2O_3 Catalysts for Liquid-Phase Hydrogenation: The Influence of the Pd : Cu Ratio on the Structure and Catalytic Characteristics

P. V. Markov[a], G. O. Bragina[a], G. N. Baeva[a], A. V. Rassolov[a], I. S. Mashkovsky[a, *], and A. Yu. Stakheev[a, **]

[a]*Zelinsky Institute of Organic Chemistry, Russian Academy of Sciences, Moscow, 119991 Russia*

**e-mail: im@ioc.ac.ru*

***e-mail: st@ioc.ac.ru*

Received March 3, 2018

Abstract—The structure and catalytic characteristics of a series of Pd–Cu/α-Al_2O_3 catalysts with Pd : Cu ratio varied from Pd_1–$Cu_{0.5}$ to Pd_1–Cu_4 were studied. The use of α-Al_2O_3 with a small surface area (S_{sp} = 8 m^2/g) as a support made it possible to minimize the effect of diffusion on the catalytic characteristics and to study the structure of Pd–Cu nanoparticles by X-ray diffraction (XRD) analysis. The XRD analysis and transmission electron microscopy (TEM) data indicated the formation of uniform bimetallic Pd–Cu nanoparticles (d = 20–60 nm), whose composition corresponded to a ratio between the metals in the catalyst, and also the absence of monometallic Pd^0 and Cu^0 nanoparticles. The study of catalytic properties in the liquid-phase hydrogenation of diphenylacetylene (DPA) showed that the activity of the catalysts rapidly decreased with the Cu content increase; however, in this case, the yield of a desired alkene compound significantly increased. The selectivity of alkene formation on the catalysts with the ratios Pd : Cu = 1 : 3 and 1 : 4 was superior to the commercial Lindlar catalyst.

Keywords: Pd–Cu, liquid-phase hydrogenation, bimetallic catalysts, nanoparticles, catalyst structure, TEM, XRD analysis, selective hydrogenation, alkynes, Lindlar catalyst

DOI: 10.1134/S0023158418050105

INTRODUCTION

The selective hydrogenation of alkyne compounds is of great practical and theoretical interest because it is used in both industrial basic and fine organic synthesis and in the laboratory practice [1]. The large-scale processes of the catalytic removal of the acetylene impurities and its homologues from ethane–ethylene fractions and the removal of phenylacetylene from styrene can serve as characteristic examples. The olefin compounds thus purified are used for the subsequent polymerization. The above impurities are strong deactivating agents because they block the active centers of polymerization catalysts (in particular, Ziegler–Natta catalysts); therefore, their concentration should be no higher than 1 ppm. In industry acetylene impurities are removed by catalytic hydrogenation in the presence of supported metal catalysts based on Ni, Ag, Au, or Cu [2–5]. However, the application of the above systems is economically unfavorable because of a number of disadvantages, such as high activation and operation temperatures and a tendency toward the intensified formation of oligomers, which deactivate the catalyst. Catalysts based on Pd possess significant activity even at low temperatures; however, they are insufficiently selective and capable of the formation of hydride phases, which considerably decreases selectivity for target olefins [6].

A promising way of developing effective catalysts for the selective hydrogenation of alkynes is the modification of Pd-containing systems with a second metal. It was shown in the literature that the use of catalysts based on Pd–Ag [7, 8], Pd–Ga [8], Pd–Zn [8, 9], Pd–Au [10], and Pd–Fe [11] makes it possible to substantially increase selectivity for the formation of olefins. Catalysts based on the bimetallic Pd–Cu compositions, which are widely used for the hydrogenation of different substrates, deserve special attention [12–15]. The properties of Pd–Cu in the gas-phase hydrogenation of acetylene in a mixture with ethylene were studied [16, 17]. A series of catalysts with different Cu : Pd ratios, in which copper serves as a structural diluent, was synthesized. It was established that, at high Cu : Pd ratios, so-called single-atom structures were formed, in which Pd atoms were completely isolated by Cu atoms, and they could be the centers of hydrogen activation; in this case, the reaction occurred on the surface of copper metal. Thus, extremely high selectivity for alkene formation, which

is characteristic of copper metal, was reached, and the presence of palladium substantially accelerated the process [17–19].

Another important area of application of selective bimetallic hydrogenation catalysts includes reactions in a liquid phase. Thus, the catalytic liquid-phase hydrogenation of disubstituted alkynes is of fundamental importance for fine organic synthesis because the hydrogenation products—*cis*- and *trans*-alkenes—are initial components for a wide range of reactions. As a rule, a commercial Lindlar catalyst, which is highly selective for *cis*-alkenes [20, 21], is currently used for C≡C bond hydrogenation in a liquid phase; however, it is insufficiently effective in the hydrogenation of substrates with triple bonds in a terminal position, and the presence of toxic lead salts in its composition restricts its applications for pharmaceutical and food industries. Furthermore, the instability of Lindlar catalyst operation under experimental conditions was noted [22].

A number of publications appeared in recent years whose authors considered the Pd–Cu catalytic systems as a possible alternative to the Lindlar catalyst for use in liquid-phase processes. Thus, Liu et al. [23] studied the properties of the synthesized Pd–Cu/C systems in the hydrogenation of a series of different substrates. In all cases, selectivity was higher than 80% in the region of high conversions, whereas the selectivity of the commercial Lindlar catalyst considerably decreased with increasing alkyne conversion. For example, the Lindlar catalyst selectivity was 46% at a phenylacetylene conversion of >90%, whereas its value varied from 80 to 90% in the Pd–Cu/C samples depending on the Cu content [23]. In our recent publications [24–26], the catalytic properties of the supported Pd–Cu catalysts in the liquid-phase hydrogenation of diphenylacetylene (DPA) were reported. The synthesized Pd–Cu systems possessed substantially higher selectivity with a maximum yield of diphenylethylene (up to 80–95%) in comparison with that of the monometallic samples.

The Pd : Cu ratio is a key factor responsible for the properties of the Pd–Cu catalysts, and changes in this ratio make it possible to regulate the catalyst activity/selectivity in gas-phase processes [16, 18]. However, the effect of this parameter on the properties of the Pd–Cu catalytic systems in liquid-phase hydrogenation remains almost unknown. In this connection, the basic task of this work consisted in a study of the dependence of the characteristics of Pd–Cu catalysts on the Pd : Cu ratio in the liquid-phase selective hydrogenation of alkynes using diphenylacetylene as a test molecule. Wide-porous α-Al_2O_3 with a small specific surface area was used for the preparation of catalysts because the effect of diffusion should be minimized for determining a relationship between the composition of bimetallic nanoparticles and their catalytic characteristics in liquid-phase reactions. This catalyst support is thermodynamically stable, and its surface is wet well with both polar and nonpolar solvents [27]. Furthermore, the high degree of crystallinity of α-Al_2O_3 made it possible to study in detail the structure of the resulting bimetallic particles by X-ray diffraction (XRD) analysis.

EXPERIMENTAL

Catalyst Preparation

The Pd–Cu/α-Al_2O_3 bimetallic catalysts were obtained by the incipient wetness impregnation of α-Al_2O_3 (Alfa Aesar, $S_{sp} = 8$ m^2/g), which was preliminarily calcined in a flow of air (550°C), with the solutions of 10% $Pd(NO_3)_2$/10% HNO_3 and $Cu(NO_3)_2 \cdot 3H_2O$. After drying, the catalyst samples were calcined in a flow of air (550°C, 4 h) and activated in a flow of 5 vol % H_2/Ar (550°C, 1 h). A commercial gas mixture from Linde Gas Rus was used for the activation. The palladium content of all of the catalysts was constant (3 wt % Pd), whereas the quantity of Cu was varied over a wide range from 0.9 to 7.2 wt %. Thus, the mole fraction of Cu (X_{Cu}) in the catalyst composition varied from 0.33 to 0.8, and the ratio Cu : Pd varied from 0.5 to 4.0. In accordance with the ratios Cu : Pd, the catalysts were designated from $Pd_1Cu_{0.5}$ to Pd_1Cu_4 (Table 1). A 3% Pd/α-Al_2O_3 reference catalyst was also prepared according to the described procedure. A commercial Lindlar catalyst (Aldrich) served as an additional reference sample.

Electron Microscopy

The catalysts were studied by transmission electron microscopy (TEM) on an HT7700 instrument (Hitachi, Japan). The analytical measurements were optimized within the framework of an approach described earlier [28]. Before taking images, powdered samples were applied from a suspension in isopropanol onto copper gauze with a diameter of 3 mm covered with a carbon film. The images were obtained in the bright-field regime at an accelerating voltage of 100 kV. The average size of nanoparticles was determined by a graphic method based on the measurement of 200–300 particles in the micrographs of different sample sections.

X-ray Diffraction Analysis

The diffractograms of the samples were measured on a D8 Advance diffractometer (Bruker, Germany; CuK_α, Ni filter, LYNXEYE detector, reflection geometry). The identification of peaks was performed using the PDF-2 2014 database. The experiment was described in detail elsewhere [29]. The composition of alloy particles was calculated using the Vegard's law based on the crystal lattice parameters of the bimetallic Pd–Cu particles [30].

Table 1. Kinetic characteristics of the selective hydrogenation of DPA on the Pd–Cu/α-Al_2O_3 catalysts with different Pd : Cu ratios

Catalyst composition	$X_{Cu/Pd}$	$r_1 \times 10^{-3}$	$r_2 \times 10^{-3}$	TOF_1	TOF_2	TOF_1/TOF_2
		mmol/min		s^{-1}		
Pd	0	43.89	6.21	0.52	0.073	7.12
$Pd_1–Cu_{0.5}$	0.33	17.91	2.72	0.10	0.016	6.25
$Pd_1–Cu_{0.67}$	0.4	14.65	2.71	0.087	0.016	5.44
$Pd_1–Cu_1$	0.5	8.38	1.52	0.049	0.009	5.44
$Pd_1–Cu_{1.5}$	0.6	6.49	0.86	0.037	0.005	7.40
$Pd_1–Cu_2$	0.67	2.57	0.31	0.015	0.002	7.50
$Pd_1–Cu_3$	0.75	0.93	0.15	0.0055	0.0009	6.11
$Pd_1–Cu_4$	0.8	1.13	0.15	0.0066	0.0009	7.33
Cu	1	0	0	0	0	0

Reaction conditions: P = 5 bar; T = 25°C; m_{Cat} = 5 mg (in the case of Pd/Al_2O_3 and Cu/Al_2O_3) or 10 mg (in the case of $Pd_1–Cu_x/Al_2O_3$); solvent, *n*-hexane.

Catalytic Tests

The liquid-phase hydrogenation of diphenylacetylene (DPA) (98%, Aldrich) in *n*-hexane (98%, Merk) was conducted in an autoclave-type catalytic setup at 25°C and a hydrogen pressure of 5 bar. The amount of hydrogen absorbed in the reaction was evaluated from a pressure drop in the reactor measured using an electronic pressure sensor. The catalyst sample weight and the intensity of stirring were chosen previously in order to ensure the occurrence of the process in the kinetic regime [24].

The hydrogenation of alkyne compounds occurs in two stages: at the first stage, the hydrogenation of parent DPA to stilbene predominantly occurs, and the complete hydrogenation product—diphenylethane—is formed at the second stage. The reaction rate r (mol_{H_2}/min) for each stage was determined from a graph of the dependence of the quantity of absorbed hydrogen on the reaction time. The specific activity of the test catalysts was evaluated based on the turnover number TOF (s^{-1}). Taking into account that it is impossible to determine the number of surface Pd atoms in a bimetallic particle by electron microscopy, the specific activity values were calculated based on the total number of palladium atoms in a catalyst sample according to the formula $TOF = r/N_{Pd}$.

The reaction mixture was analyzed by chromatography on a Crystall 5000 instrument (Chromatek, Russia) with a flame-ionization detector. The mixture components were separated on an HP5-MS column (5% phenyldimethylsiloxane; 30 m; internal diameter, 0.25 mm; stationary phase film thickness, 0.25 μm; carrier gas, helium). Selectivity for olefin formation ($S_=$) was calculated based on the results of analysis as $S_= = n_=/(n_= + n_-)$, where $n_=$ and n_- are the mole fractions of the resulting olefin and alkane, respectively.

RESULTS AND DISCUSSION

X-ray Diffraction Analysis

The study of alloy formation in supported bimetallic catalysts and the determination of the structure of bimetallic nanoparticles is a very complex problem because, as a rule, a number of factors limit the application of X-ray diffraction analysis. On the one hand, this is related to the broadening and low intensity of the diffraction peaks of a metal phase because of the small size of the metal nanoparticles and, on the other hand, to their overlapping with signals from the support [31]. In order to avoid these limitations, we used α-Al_2O_3 as a support in this work. Because of the high degree of crystallinity of this support, its diffraction peaks possess small width and high symmetry, which makes it possible to minimize the overlapping of signals corresponded to the support and the metal nanoparticles.

Figure 1 illustrates the results of the structure characterization of the bimetallic Pd–Cu catalysts by XRD analysis and also shows the diffractograms of the monometallic (*1*) $Pd/α$-Al_2O_3 and (*7*) $Cu/α$-Al_2O_3 samples and (*8*) the initial support.

The diffractogram of the initial carrier contains two high-intensity peaks at $2\theta \approx 37.6°$ and 43.2°, which are characteristic of α-Al_2O_3 [32]. In the diffractogram of the monometallic $Pd/α$-Al_2O_3 sample, two broad peaks at $2\theta \approx 40°$ and 46.5°, which correspond to Pd(111) and Pd(200), respectively [33], are observed in addition to the reflections of the initial support. Note that the $Cu/α$-Al_2O_3 sample exhibited a low-intensity reflection at $2\theta \approx 50.2°$ due to Cu(200). An intense peak of Cu(111) at $2\theta = 43.3°$ [34] is inaccessible for identification because its major portion overlaps with the signal of the initial α-Al_2O_3.

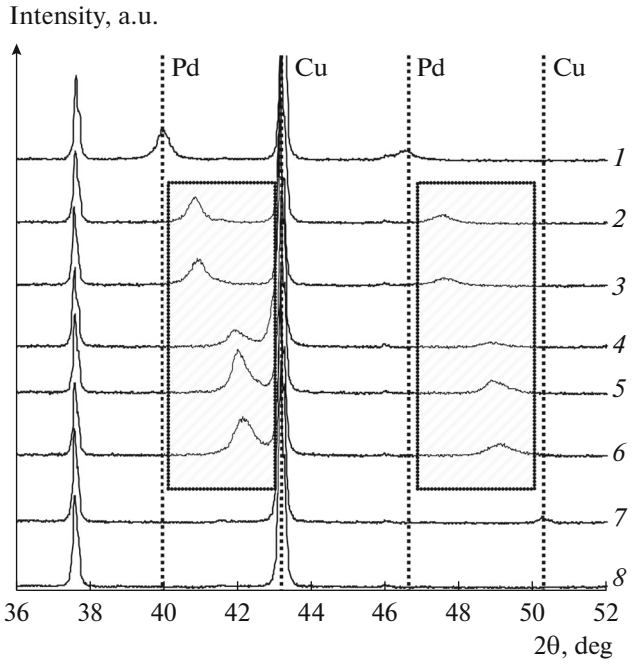

Fig. 1. Diffractograms of the monometallic (*1*) Pd/α-Al_2O_3 and (*7*) Cu/α-Al_2O_3 catalysts and the bimetallic (*2*) Pd_1–$Cu_{0.5}$, (*3*) Pd_1–Cu_1, (*4*) Pd_1–Cu_2, (*5*) Pd_1–Cu_3, and (*6*) Pd_1–Cu_4 catalysts. For comparison, a diffractogram of (*8*) the initial α-Al_2O_3 support is shown. The regions of the formation of Pd–Cu particles are shown by hatching.

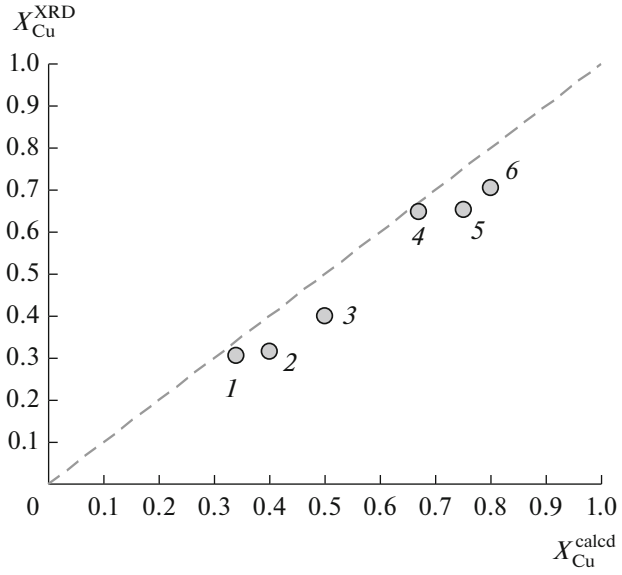

Fig. 2. Composition of the bimetallic samples of (*1*) Pd_1–$Cu_{0.5}$, (*2*) Pd_1–$Cu_{0.67}$, (*3*) Pd_1–Cu_1, (*4*) Pd_1–Cu_2, (*5*) Pd_1–Cu_3, and (*6*) Pd_1–Cu_4 determined according to the Vegard's law. The dashed line describes the composition of samples calculated at the stage of preparation. X_{Cu}^{calcd} is the fraction of Cu according to calculation data, and X_{Cu}^{XRD} is the fraction of Cu according to XRD analysis data.

In the diffractograms of the bimetallic catalysts, signals characteristic of Pd–Cu(111) and Pd–Cu(200) were detected in the regions of ~41°–42.8° and ~47°–50°, respectively [23, 35]. An analysis of the diffractograms showed that the positions of Bragg reflections shifted from the values of 2θ characteristic of Pd^0 toward greater angles with increasing the copper content; this was caused by a decrease in the lattice parameter as a result of the substitution of smaller Cu atoms for a portion of palladium atoms. The observed change in the intensity of Pd–Cu(111) signals can be related to both a change in the particle-size distribution of bimetallic nanoparticles and a change in the degree of ordering of the crystal structure of Pd–Cu nanoparticles. The observed shift of the peak of Pd(111) makes it possible to quantitatively analyze the composition of the resulting nanoparticles using the Vegard's law [36], according to which the crystal lattice parameter *a* of alloy linearly depends on the molar concentration of a component. Based on calculations, we found that the molar fraction of Cu in the Pd–Cu nanoparticles was close to the molar fraction of copper in the catalyst (Fig. 2). The experimental data are indicative of the formation of Pd–Cu substitution alloy with a hexagonal face-centered crystal lattice structure [37, 38], and allowed us to conclude that both of the metals completely included into the composition of the alloy without the formation of monometallic nanoparticles. This was confirmed by the absence of signals characteristic of Pd^0 and Cu^0 from the diffractograms of the bimetallic samples. Note that the peaks of both the monometallic Pd/α-Al_2O_3 and the bimetallic Pd–Cu/α-Al_2O_3 catalysts were symmetrical regularly shaped; this fact indicated the ordering of the alloy structure and the uniformity of the composition of bimetallic nanoparticles formed [39].

Transmission Electron Microscopy

Figure 3 shows the TEM micrographs of the bimetallic test samples and the histograms of particle size distributions. The micrographs clearly indicate that nanoparticles in the Pd_1–$Cu_{0.5}$, Pd_1–Cu_1, and Pd_1–$Cu_{1.5}$ samples were somewhat flattened in shape and unevenly distributed over the support surface (Figs. 3a–3c). They were also characterized by a wide modal particle-size distribution in a range from 10 to 110 nm. An analysis of the bar diagrams allowed us to conclude that particles with average sizes of 60, 69, and 54 nm were formed the Pd_1–$Cu_{0.5}$, Pd_1–Cu_1, and Pd_1–$Cu_{1.5}$ samples, respectively. Note that a considerable fraction of the surface was occupied by larger agglomerates (70–100 nm).

The particle-size distribution of metallic nanoparticles somewhat changed as the copper content was increased. The bimetallic particles detected in the Pd_1–Cu_2 sample (not shown in Fig. 3) were nearly

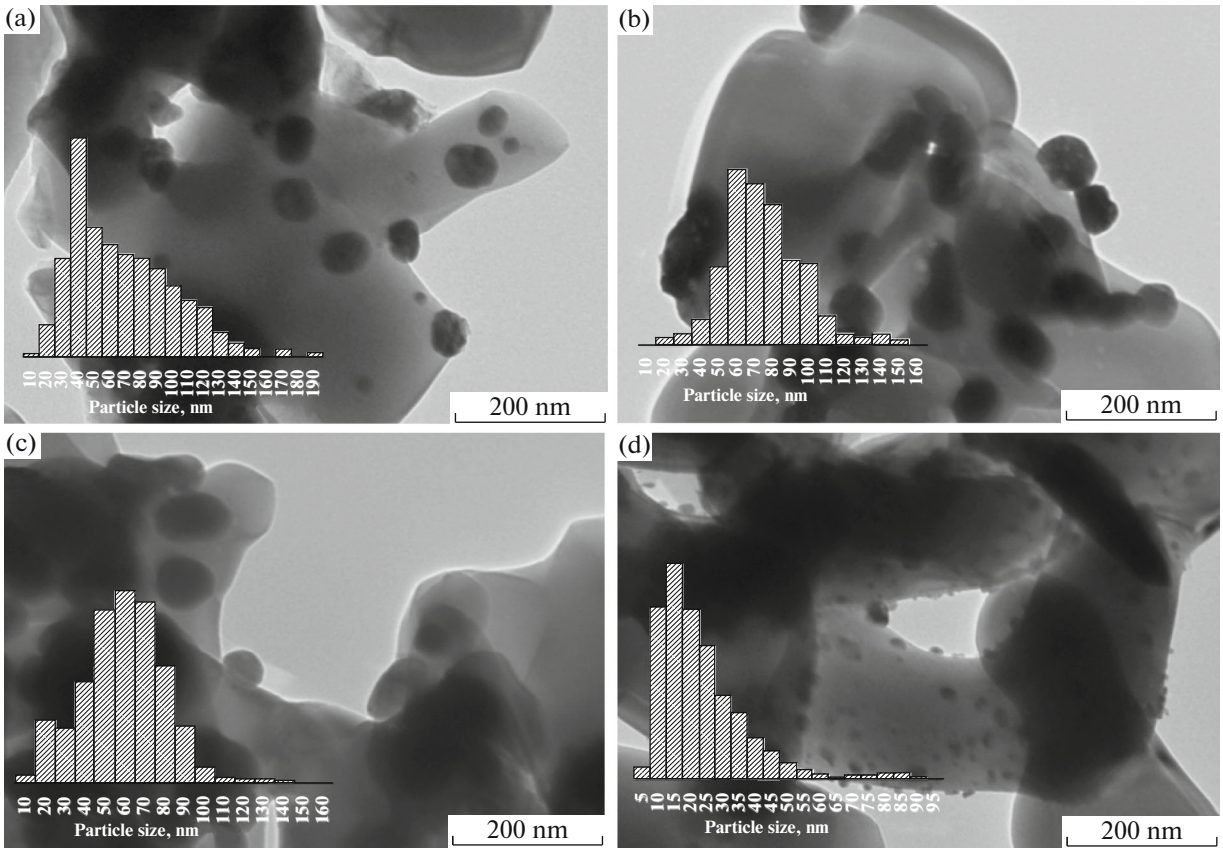

Fig. 3. TEM micrographs of the Pd–Cu/Al_2O_3 catalysts: (a) Pd_1–$Cu_{0.5}$, (b) Pd_1–Cu_1, (c) Pd_1–$Cu_{1,5}$, and (d) Pd_1–Cu_3.

spherical in shape and more uniformly distributed over the surface in comparison with those in the samples described above. The distribution histogram is centered at 30 nm; at the same time, larger particles also occurred on the surface.

A further increase in the copper content (the Pd_1–Cu_3 sample, Fig. 3d) led to a certain decrease in the diameter of Pd–Cu nanoparticles, whose average size was ~20 nm. The structure of the samples was ordered; the particles were spherically shaped and evenly distributed over the surface, and large agglomerates were almost absent.

Selective Hydrogenation of Diphenylacetylene

Activity of Pd–Cu catalysts in the hydrogenation of diphenylacetylene. Figure 4 shows the kinetic curves of hydrogen absorption in the hydrogenation of diphenylacetylene (DPA) on Pd/Al_2O_3 and the Pd–Cu/Al_2O_3 catalysts with different Pd : Cu ratios, and Table 1 summarizes the rates of hydrogenation at the first and second stages of the process. The kinetic curves obtained for all of the above samples exhibit an characteristic bend after the absorption of 1 equiv of H_2, which is indicative of the inhibition of hydrogenation on going from the first (C≡C bond hydrogenation) to the second (C=C bond hydrogenation) stage of the process. These results are consistent with published data on the hydrogenation of DPA on Pd catalysts [40, 41]. The activity of the Cu/Al_2O_3 reference catalyst was negligibly small, and the absorption of hydrogen was not observed.

The rate of hydrogenation on the Pd catalyst was noticeably higher than that on the samples modified with copper; in this case, a pronounced correlation between the quantity of copper in the catalyst and the rate of hydrogenation was observed: the rate of the process rapidly decreased with increasing the Cu content. To analyze the effect of the Cu content on the catalyst activity, we calculated the values of TOF_1 and TOF_2 based on the total Pd amount in the sample (Table 1). Figure 5 shows the dependence of TOF_1 on the mole fraction Cu in the bimetallic nanoparticles. It is evident that the introduction of even a relatively small quantity of copper (the Pd_1–$Cu_{0.5}$ catalyst) led to a sharp drop in the activity (TOF_1 changed from 0.5 to 0.1 s^{-1}), and the activity continued to decrease but more smoothly with a further increase in the Cu content.

Similar results were obtained in a number of studies on the activity of Pd–Cu catalysts in gas-phase hydro-

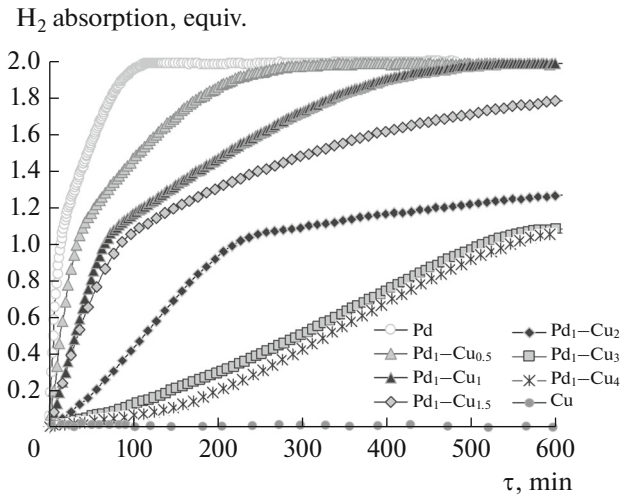

Fig. 4. Dependence of the equivalent quantity of absorbed hydrogen on the reaction time of DPA hydrogenation on the catalysts with different Cu : Pd ratios. Reaction conditions: $P = 5$ bar; $T = 25°C$; $m_{Cat} = 5$ mg (in the case of Pd/Al_2O_3 and Cu/Al_2O_3) or 10 mg (in the case of $Pd_1–Cu_x$/Al2O3); solvent, *n*-hexane.

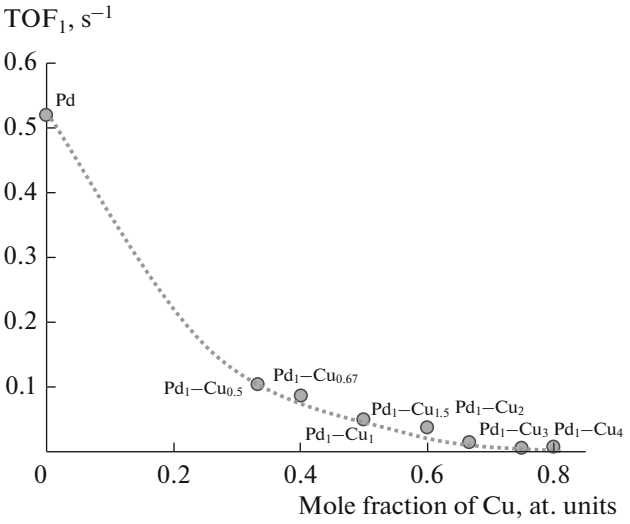

Fig. 5. Dependence of the specific catalytic activity at the first stage of hydrogenation (TOF_1) on the mole fraction of Cu in the Pd–Cu nanoparticles.

genation processes [14, 18, 26]. A decrease in the activity of Pd catalysts upon their modification with Cu is primarily related to the fact that a portion of surface palladium atoms, on which hydrogenation occurs, in the bimetallic samples is replaced by the Cu atoms, which does not possess catalytic activity in the reaction in question. Furthermore, the surface of metallic particles can be additionally enriched in copper as a result of its surface segregation, which is a thermodynamically favorable process [42, 43]. Thus, Cheng et al. [44] used the Monte Carlo method to demonstrate that the single atoms and the mono-, di-, and trimeric Pd ensembles surrounded by surface Cu atoms, whose properties differ significantly from the properties of pure metals, can be formed as a result of the segregations of copper on the surface of bimetallic particles. The effect of the segregation of copper onto the surface of bimetallic Pd–Cu particles was also observed previously for the $Pd–Cu/Al_2O_3$ catalysts obtained from heterobimetallic Pd–Cu acetate complexes [26]. An analogous effect was found on the modification of palladium catalysts with In, Ag, and Zn [45–47]. The fact that the addition of even insignificant quantities of copper leads to a sharp decrease in activity indirectly indicates the effect of the surface segregation of copper on the catalytic characteristics of the test samples because the number of active Pd centers on which the reaction occurs decreases to a larger degree.

Selectivity for the formation of diphenylethylene (DPE). Figure 6 shows the dependences of the composition of hydrogenation products on reaction time for the $Pd_1–Cu_{0.5}$, $Pd_1–Cu_{1.5}$, and $Pd_1–Cu_3$ catalysts and the monometallic Pd reference sample. The volcano-like shape of the curve that characterizes the amount of DPE formed is consistent with the consecutive reaction mechanism of the hydrogenation of alkynes, in accordance with which triple bond hydrogenation occurs at the first stage with the formation of an alkene intermediate with following conversion to alkane at the second stage. An analysis of the dependences given in Fig. 6 allowed us to conclude that the maximum yield of the desired alkene compound gradually increased with Cu content of Pd–Cu nanoparticles from ~81% on monometallic $Pd/\alpha\text{-}Al_2O_3$ to 92–93% on the bimetallic $Pd_1–Cu_3/\alpha\text{-}Al_2O_3$ sample.

A lower concentration of diphenylethane (DPEt) formed at the first stage of the process also indicates an increase in the selectivity of Pd–Cu catalysts. Thus, in the reaction performed on $Pd/\alpha\text{-}Al_2O_3$, DPEt appeared in noticeable quantities even at low degrees of DPA conversion, and its concentration was higher than 20–25% after complete alkyne hydrogenation (Fig. 6a). For the Pd–Cu samples, the concentration of diphenylethane formed at the first stage in the presence of alkyne systematically decreased with the copper content increase, and it was no higher than 5–6% after complete DPA hydrogenation on the $Pd_1–Cu_3$ catalyst (Fig. 6d). The experimental data indicate that the contribution of a complete hydrogenation reaction, which occurs simultaneously with a partial hydrogenation reaction, to the overall process decreased with increasing the copper content to cause an increase in the yield of the desired alkene intermediate and, consecutively, in the process selectivity.

Figure 7 shows the dependence of selectivity for the formation of diphenylethylene on the conversion of diphenylacetylene for the monometallic $Pd/\alpha\text{-}Al_2O_3$

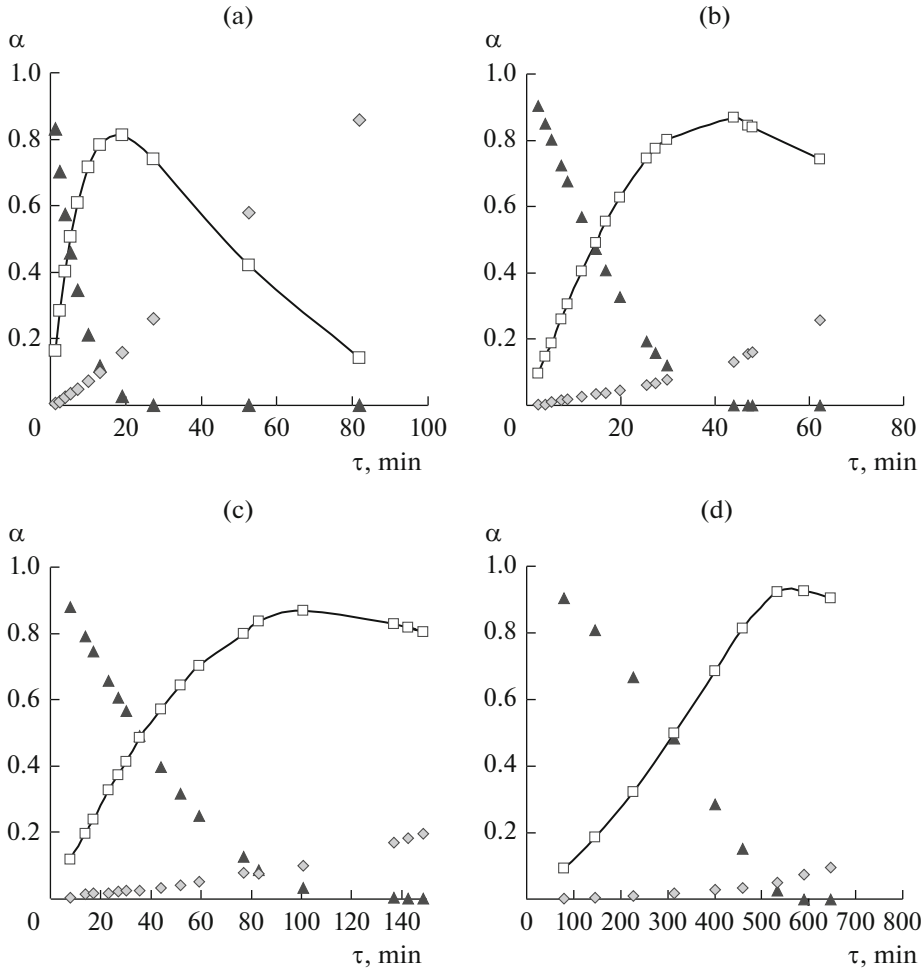

Fig. 6. Composition of the reaction products of the selective hydrogenation of DPA on the (a) Pd/Al_2O_3, (b) $Pd_1–Cu_{0.5}$, (c) $Pd_1–Cu_{1.5}$, and (d) $Pd_1–Cu_3$ catalysts: (▲) diphenylacetylene, (□) diphenylethylene, and (◇) diphenylethane.

sample and the bimetallic catalysts with different Pd : Cu ratios. For comparison, the graph also shows data obtained on the commercial Lindlar catalyst. At a DPA conversion of ~16%, the selectivity of the Pd/α-Al_2O_3 catalyst for olefin formation was 96%, and this value substantially decreased with the conversion. Taking into account the two-stage mechanism of the hydrogenation reaction proposed by Bond et al. [48], which was adapted for liquid-phase processes [48, 49], we hypothesized that selectivity decreased as a result of the strong adsorption of DPE on the surface of Pd nanoparticles. On the one hand, this led to the fact that, with an increase in the concentration of DPE in the solution, its quantity on the catalyst surface also increased as a result of competitive adsorption; therefore, the rate of the alkane formation increased. On the other hand, when the strength of DPE adsorption increases, the heat of its desorption became higher than the activation energy of the second stage of hydrogenation, thus reducing the probability of DPE desorption and increasing the probability of its hydrogenation [50].

Upon the modification of a catalyst with copper, its selectivity for olefin considerably increased, as compared with that of a monometallic analog, and its value increased with the copper content of the catalysts. This result is consistent with published data obtained in a study of the gas-phase hydrogenation of acetylene in the presence of an excess of ethylene [16, 18]. The dependence of selectivity for olefin formation ($S_=$) on the conversion of DPA (X_{DPA}) is linear at $X_{DPA} < 50\%$. The selectivity of the catalysts modified with copper gradually decreased with increasing conversion; however, its values are higher than those of the monometallic sample. Thus, at a DPA conversion of >95%, the value of S_{DPE} for Pd/α-Al_2O_3 was ~83%, whereas the value of this parameter was ~94–95% for $Pd_1–Cu_3$ and $Pd_1–Cu_4$. The $Pd_1–Cu_3$ and $Pd_1–Cu_4$ catalysts were superior to the Lindlar catalyst in terms of selectivity in the region of high conversions; therefore, the Pd–Cu system can be consider as a possible

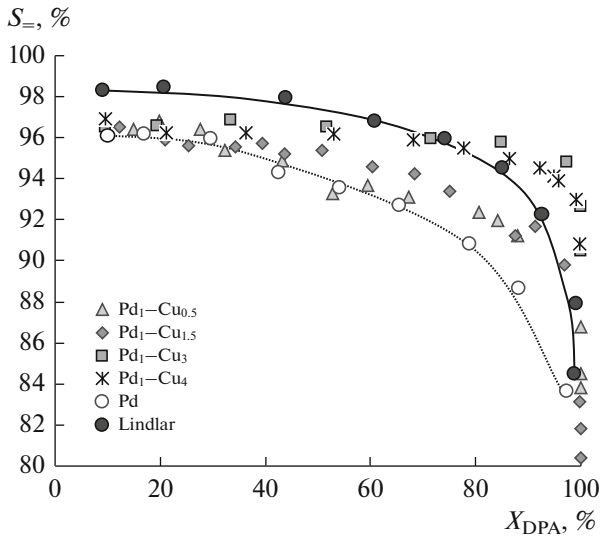

Fig. 7. Dependence of selectivity for diphenylethylene formation ($S_=$) on the conversion of diphenylacetylene for the $Pd–Cu/Al_2O_3$ catalysts with different copper contents.

alternative for the commercial sample. Note that all of the synthesized catalysts possessed extremely high (>95%) selectivity for the formation of *cis*-alkenes; this fact is consistent with published data on the hydrogenation of DPA [51–53].

Thus, the experimental data indicate that the rate of hydrogenation slowed down and the process selectivity increased with the copper content of the Pd–Cu nanoparticles. The observed increase in the selectivity was related to a decrease in the heat of adsorption of the alkene intermediate as a result of a decrease in the electron density on the surface atoms of Pd, as demonstrated previously by the IR spectroscopy of adsorbed CO [25]. Furthermore, upon the formation of Pd–Cu alloy, the quantity of di- or triatomic active centers of palladium, at which molecules with double C=C bonds are adsorbed more strongly than at the centers formed by single Pd atoms, decreased [16, 18]. As a result, the probability of DPE desorption without further hydrogenation increased; therefore, the selectivity of the Pd–Cu catalyst remained high until the complete conversion of DPA. The suppression of the formation of palladium hydride PdH_x [54, 55] can also facilitate an increase in the selectivity of the bimetallic catalysts, as found earlier for the catalysts based on Pd–In [24] and Pd–Zn [47].

CONCLUSIONS

Thus, in the course of this study, we examined in detail the effect of the Pd : Cu ratio over a wide range (from 2 : 1 to 1 : 4) on the activity and selectivity of bimetallic Pd–Cu catalysts in the liquid-phase hydrogenation of diphenylacetylene. The use of α-Al_2O_3 as a support allowed us to determine the structure and composition of Pd–Cu nanoparticles using XRD analysis and to minimize the influence of diffusion on the kinetics of hydrogenation. The catalytic data showed that the selectivity of the catalysts for the formation of intermediate hydrogenation products considerably increased because of the formation of Pd–Cu alloy, which was accompanied by a decrease in the catalyst activity. We found that the catalysts with high copper content (Pd : Cu = 1 : 3 and 1 : 4) were superior to the commercial Lindlar catalyst in terms of selectivity.

ACKNOWLEDGMENTS

We are grateful to the Department of Structural Studies of the Zelinsky Institute of Organic Chemistry, Russian Academy of Sciences, for studying the samples by electron microscopy. This work was supported by the Russian Science Foundation (grant no. 16-13-10530).

REFERENCES

1. Blaser, H.-U., Schnyder, A., Steiner, H., Rössler, F., and Baumeister, P., *Handbook of Heterogeneous Catalysis*, Knözinger, H., Scheth, F., and Weitkamp, J., Eds., Wiley-VCH, 2008.
2. Vile, G., Albani, D., Almora-Barrios, N., López, N., and Pérez-Ramírez, J., *ChemCatChem*, 2016, vol. 8, p. 21.
3. Bridier, B., Hevia, M.A.G., López, N., and Pérez-Ramírez, J., *J. Catal.*, 2010, vol. 278, p. 167.
4. Liu, X., Mou, C.-Y., Lee, S., Li, Y., Secrest, J., and Jang, B.W.-L., *J. Catal.*, 2012, vol. 285, p. 152.
5. Trimm, D.L., Cant, N.W., and Liu, I.O.Y., *Catal. Today*, 2011, vol. 178, p. 181.
6. Molnár, Á., Sárkány, A., and Varga, M., *J. Mol. Catal.*, 2001, vol. 173, p. 185.
7. Chesnokov, V.V., Chichkan', A.S., and Ismagilov, Z.R., *Kinet. Catal.*, 2017, vol. 58, no. 5, p. 649.
8. Glyzdova, D.V., Smirnova, N.S., Shlyapin, D.A., Tsyrul'nikov, P.G., Leont'eva, N.N., Vershinin, V.I., Gerasimov, E.Y., and Prosvirin, I.P., *Kinet. Catal.*, 2017, vol. 58, no. 2, p. 140.
9. Okhlopkova, L.B., Cherepanova, S.V., Prosvirin, I.P., Kerzhentsev, M.A., and Ismagilov, Z.R., *Appl. Catal., A*, vol. 549, p. 245.
10. Nikolaev, S.A. and Krotova, I.N., *Pet. Chem.*, 2013, vol. 53, no. 6, p. 394.
11. Shesterkina, A.A., Kozlova, L.M., Kirichenko, O.A., Kapustin, G.I., Mishin, I.V., and Kustov, L.M., *Rus. Chem. Bull.*, 2016, vol. 65, no. 2, p. 432.
12. Furlong, B.K., Hightower, J.W., Chan, T.Y.-L., Sarkany, A., and Guczi, L., *Appl. Catal., A*, 1994, vol. 117, p. 41.
13. Benedetti, A., Fagherazzi, G., Pinna, F., Rampazzo, G., Selva, M., and Strukul, G., *Catal. Lett.*, 1991, vol. 10, p. 215.
14. Guczi, L., Schay, Z., Stefler, Gy., Liotta, L.F., Deganello, G., and Venezia, A.M., *J. Catal.*, 1999, vol. 182, p. 456.

15. Nosova, L.V., Zaikovskii, V.I., Kalinkin, A.V., Talzi, E.P., Paukshtis, E.A., and Ryndin, Y.A., *Kinet. Catal.*, 1995, vol. 36, no. 3., p. 328.
16. McCue, A.J., Shepherd, A.M., and Anderson, J.A., *Catal. Sci. Technol.*, 2015, vol. 5, p. 2880.
17. Zhang, R., Zhang, J., Zhao, B., He, L., Wang, A., and Wang, B., *J. Phys. Chem. C*, 2017, vol. 121, no. 50, p. 27936.
18. McCue, A.J., McRitchie, C.J., Shepherd, A.M., and Anderson, L.A., *J. Catal.*, 2014, vol. 319, p. 127.
19. Yang, K. and Yang, B., *Phys. Chem. Chem. Phys.*, 2017, vol. 19, p. 18010.
20. Lindlar, H. and Dubuis, R., *Org. Synth.*, 1966, vol. 46, p. 89.
21. Rajaram, J., Narula, A.P.S., Chawla, H.P.S., and Dev, S., *Tetrahedron*, 1983, vol. 39, p. 2315.
22. Mitsudome, T., Takahashi, Y., Ichikawa, S., Mizugaki, T., Jitsukawa, K., and Kaneda, K., *Angew. Chem.*, 2013, vol. 52, p. 1481.
23. Liu, J., Zhu, Ya., Liu, Ch., Wang, X., Cao, Ch., and Song, W., *ChemCatChem*, 2017, vol. 9, p. 4053.
24. Markov, P.V., Bragina, G.O., Baeva, G.N., Tkachenko, O.P., Mashkovsky, I.S., Yakushev, I.A., Kozitsyna, N.Y., Vargaftik, M.N., and Stakheev, A.Y., *Kinet. Catal.*, 2015, vol. 56, no. 5, p. 591.
25. Mashkovsky, I.S., Markov, P.V., Bragina, G.O., Tkachenko, O.P., Stakheev, A.Y., Yakushev, I.A., Kozitsyna, N.Y., and Vargaftik, M.N., *Russ. Chem. Bull.*, 2016, no. 2, p. 425.
26. Markov, P.V., Bragina, G.O., Rassolov, A.V., Baeva, G.N., Mashkovsky, I.S., Murzin, V.Yu., Zubavichus, Ya.V., and Stakheev, A.Yu., *Mendeleev Commun.*, 2016, vol. 26, no. 6, p. 502.
27. Satterfield, C.N., *Heterogeneous Catalysis in Practice*, New York: McGraw-Hill, 1980.
28. Kachala, V.V., Khemchyan, L.L., Kashin, A.S., Orlov, N.V., Grachev, A.A., Zalesskiy, S.S., and Ananikov, V.P., *Rus. Chem. Rev.*, 2013, vol. 82, no. 7, p. 648.
29. Gavrikov, A.V., Koroteev, P.S., Dobrokhotova, Zh.V., Ilyukhin, A.B., Efimov, N.N., Kirdyankin, D.I., Bykov, M.A., Ryumin, M.A., and Novotortsev, V.M., *Polyhedron*, 2015, vol. 102, p. 4.
30. Bagmut, A.G., Shipkova, I.G., and Zhuchkov, V.A., *J. Surf. Invest.: X-Ray, Synchrotron Neutron Tech.*, 2011, vol. 5, no. 3, p. 460.
31. Gallagher, J.R., Li, T., Zhao, H., Liu, J., Lei, Yu, Zhang, X., Ren, Ya., Elam, J.W., Meyer, R.J., Winans, R.E., and Miller, J.T., *Catal. Sci. Technol.*, 2014, vol. 4, p. 3053.
32. Kerdkool, P. and Niyomwas, S., *Procedia Eng.*, 2012, vol. 32, p. 642.
33. Yan, B., Wang, C., Xu, H., Zhang, K., Li, Sh., and Du, Yu., *ChemPlusChem*, 2017, vol. 82, p. 1121.
34. Pei, G., Liu, X., Chai, M., Wang, A., and Zhang, T., *Chin. J. Catal.*, 2017, vol. 38, p. 1540.
35. Yang, F., Zhang, Ya., Liu, P.-F., Cui, Yi., Ge, X.-R., and Jing, Q.-Sh., *Int. J. Hydrogen Energy*, 2016, vol. 41, p. 6773.
36. Denton, A. R. and Ashcroft, N. W., *Phys. Rev. A*, 1991, vol. 43, p. 3161.
37. Lv, J.-J., Lia, Sh.-Sh., Wang, A.-J., Mei, L.-P., Feng, J.-J., Chen, J.-R., and Chen, Z., J. *Power Sources*, 2014, vol. 269, p. 104.
38. Al-Mufachi, N.A. and Steinberger-Wilckens, R., *Thin Solid Films*, 2018, vol. 646, p. 83.
39. Feng, Y.-S., Liu, C., Kang, Y.-M., Zhou, X.-M., Liu, L.-L., Deng, J., Xu, H.-J., and Fu, Y., *Chem. Eng. J.*, 2015, vol. 281, p. 96.
40. Marín-Astorga, N., Alvez-Manoli, G., and Reyes, P., *J. Mol. Catal. A: Chem.*, 2005, vol. 226, p. 81.
41. Choudary, B.M., Lakshmi Kantam, M., Mahender Reddy, N., Koteswara Rao, K., Haritha, Y., Bhaskar, V., Figueras, F., and Tuel, A., *Appl. Catal., A*, 1999, vol. 181, p. 139.
42. Løvvik, O.M., *Surf. Sci.*, 2005, vol. 583, p. 100.
43. Lambert, S., Heinrichs, B., Brasseur, A., Rulmont, A., and Pirard, J.P., *Appl. Catal., A*, 2004, vol. 270, p. 201.
44. Cheng, F., He, X., Chen, Z.-X., and Huang, Y.-G., *J. Alloys Compd.*, 2015, vol. 648, p. 1090.
45. Burueva, D.B., Kovtunov, K.V., Bukhtiyarov, A.V., Barskiy, D.A., Prosvirin, I.P., Mashkovsky, I.S., Baeva, G.N., Bukhtiyarov, V.I., Stakheev, A.Yu., and Koptyug, I.V., *Chem. Eur. J.*, 2018, vol. 24, p. 2547.
46. Rassolov, A.V., Markov, P.V., Bragina, G.O., Baeva, G.N., Mashkovskii, I.S., Stakheev, A.Y., Yakushev, I.A., and Vargaftik, M.N., *Kinet. Catal.*, 2016, vol. 57, no. 6, p. 853.
47. Mashkovsky, I.S., Markov, P.V., Bragina, G.O., Baeva, G.N., Rassolov, A.V., Bukhtiyarov, A.V., Prosvirin, I.P., Bukhtiyarov, V.I., and Stakheev, A.Yu., *Mendeleev Commun.*, 2018, vol. 28, no. 2, p. 152.
48. Bond, G.C., *Metal-Catalysed Reactions of Hydrocarbons*, New York: Springer Science + Business Media Inc., 2005.
49. Markov, P.V., Bragina, G.O., Rassolov, A.V., Mashkovsky, I.S., Baeva, G.N., Tkachenko, O.P., Yakushev, I.A., Vargaftik, M.N., and Stakheev, A.Yu., *Mendeleev Commun.*, 2016, vol. 26, p. 494.
50. Studt, F., Abild-Pedersen, F., Bligaard, T., Sørensen, R.Z., Christensen, C.H., and Nørskov, J.K., *Science*, 2008, vol. 320, p. 1320.
51. Furukawa, S., Yokoyama, A., and Komatsu, T., *ACS Catal.*, 2014, vol. 4, p. 3581.
52. Komatsu, T., Takagi, K., and Ozawa, K., *Catal. Today*, 2011, vol. 164, p. 143.
53. Spee, M.P.R., Boersma, J., Meijer, M.D., Slagt, M.Q., van Koten, G., and Geus, J.W., J. *Org. Chem.*, 2011, vol. 66, p. 1647.
54. Coq, B. and Figueras, F., *J. Mol. Catal. A: Chem.*, 2011, vol. 173, p. 117
55. Armbrüster, M., Behrens, M., Cinquini, F., Föttinger, K., Grin, Yu., Haghofer, A., Klötzer, B., Knop-Gericke, A., Lorenz, H., Ota, A., Penner, S., Prinz, J., Rameshan, C., Révay, Z., Rosenthal, D., Rupprechter, G., Sautet, P., Schlögl, R., Shao, L., Szentmiklósi, L., Teschner, D., Torres, D., Wagner, R., Widmer, R., and Wowsnick, G., *ChemCatChem*, 2012, vol. 4, p. 1048.

Translated by V. Makhlyarchuk